Contribution from the W. R. Kenan, Jr. Laboratory, Department of Chemistry, The University of North Carolina, Chapel Hill, North Carolina 27514

Seven-Coordinate Tricarbonylbis(*N*,*N*-dialkyldithiocarbamato)tungsten(II) Complexes. Molecular Structure and Dynamic Properties

JOSEPH L. TEMPLETON* and BENNETT C. WARD

Received August 9, 1979

The crystal and molecular structure of tricarbonylbis(*N*,*N*-dimethyldithiocarbamato)tungsten(II) has been determined by a single-crystal X-ray diffraction study. Dynamic ^{13}C NMR studies of $W(CO)_3(S_2CNR_2)_2$ have revealed two distinct intramolecular rearrangement processes for both R = Me and R = Et. Selective averaging of two of the three distinct carbon monoxide resonances observed in the low-temperature limiting spectrum occurs initially prior to coalescence of all three carbonyl signals to produce a single ^{13}CO resonance at room temperature. Crystals of $W(CO)_3[S_2CN(CH_3)_2]_2$ were found to be monoclinic, space group $C2/c$, with a unit cell of dimensions a = 18.612 (3) Å, b = 6.313 (1) Å, c = 26.566 (5) Å, and β = 93.76 (1)°. The observed density is 2.14 (2) g cm^{-3} while a density of 2.18 g cm^{-3} is calculated for Z = 8. The structure was refined to R_1 = 0.070 and R_2 = 0.089 by using 3779 reflections with $F > 3\sigma(F)$. The tungsten is seven-coordinate with three carbonyl ligands (W–C: 1.964 (11), 1.966 (11), and 2.021 (10) Å) and two bidentate dithiocarbamate ligands (W–S: 2.501 (2), 2.523 (3), 2.538 (3), and 2.569 (3) Å) occupying the inner coordination sphere. Quantitative analysis of the observed structure reveals the coordination polyhedron of the tungsten to be best described as a 4:3 tetragonal base–trigonal base geometry. The fluxional properties exhibited by $W(CO)_3(S_2CNR_2)_2$ complexes in solution are discussed with reference to the heptacoordinate solid-state geometry determined for $W(CO)_3[S_2CN(CH_3)_2]_2$.

Introduction

The molecular structures present in the solid state and the intramolecular rearrangement processes which are exhibited in solution by seven-coordinate transition-metal complexes remain poorly understood relative to lower coordination number structures and dynamics.[1] Motivation for systematically exploring the behavior of stable seven-coordinate compounds stems not only from intrinsic interest in such higher coordination numbers but also from the role of expanded coordination spheres in associative reactions of octahedral metal complexes. Wreford's report of the preparation and isolation of the metastable *trans*-$Mo(CO)_2(dppe)_2$ isomer from the thermodynamically favored *cis*-$Mo(CO)_2(dppe)_2$ by formation of a seven-coordinate metal hydride intermediate provides an illustration of the potential stereochemical utility of seven-coordinate complexes.[2] Of current interest is the possibility that a seven-coordinate metallocyclobutane may exert stereochemical control of cyclopropane products formed when $(OC)_5W(CHPh)$ reacts with substituted alkenes.[3]

Coordination number seven dominates much of the chemistry of molybdenum(II) and tungsten(II) complexes containing carbon monoxide ligands. The abundance of these seven-coordinate compounds is consistent with the effective atomic number rule as applied to d^4 metal ions which require an additional seven electron pairs to attain a total valence electron count of eighteen. Two features which seem to permeate the chemistry of seven-coordinate complexes investigated to date include significant deviations from any idealized geometry in the solid state and facile intramolecular rearrangements in solution.

The minima associated with the potential energy surface of idealized seven-coordinate geometries are relatively shallow and suggest that intramolecular rearrangements should be facile.[4] Indeed stereochemical nonrigidity is a feature common to many seven-coordinate complexes. Several cases of polytopal isomerization amenable to dynamic NMR studies have been analyzed in detail, and mechanistic conclusions have been drawn.[5]

A large body of structural data for seven-coordinate compounds has accumulated during the past decade.[6] Structural descriptions are most often couched in terms of deviations from one of three idealized geometries [pentagonal bipyramid (D_{5h}, 1:5:1), capped octahedron (C_{3v}, 1:3:3), or capped trigonal prism (C_{2v}, 1:4:2)]. Unambiguous classification of an experimentally observed structure can be particularly difficult for complexes containing either inequivalent ligands and/or chelating ligands.[7]

A survey of X-ray data tabulated for seven-coordinate compounds[6] reveals no structural information for compounds of the type $M(CO)_3(B–B)_2$ where B–B represents a bidentate monoanionic ligand. Colton's synthesis of $Mo(CO)_3(dtc)_2$ (dtc = $R_2NCS_2^-$)[8] provides one example of a complex from this category. McDonald has prepared closely related tungsten species of the type $W(CO)_2(PPh_3)(B–B)_2$ (B–B = $^-S_2CNR_2$, ^-S_2COR, and $^-S_2P(OEt)_2$).[9] We have recently reported the synthesis of $W(CO)_3(dmtc)_2$ (dmtc = $^-S_2CNMe_2$) and investigated its dynamic ^{13}C NMR properties.[10] In this paper we report the crystal structure of tricarbonylbis(*N*,*N*-dimethyldithiocarbamato)tungsten and extend the previous preparative techniques and dynamic NMR studies to additional $W(CO)_3(dtc)_2$ complexes.

Experimental Section

Materials and Procedure. All manipulations were performed under an atmosphere of prepurified nitrogen or argon by using standard Schlenk techniques. Tetrahydrofuran and toluene were distilled from sodium benzophenone ketyl; cyclohexane was dried over molecular sieves (4 Å) and purged with a nitrogen stream prior to use; all other solvents were purged with a nitrogen stream and used without further purification. Tetracarbonyldiiodotungsten was prepared photochemically from $W(CO)_6$ and I_2 by the method of Colton and Rix.[11]

^1H NMR (100 MHz) and ^{13}C NMR (25.2 MHz) spectra were

(1) Datta, S.; Wreford, S. S. *Inorg. Chem.* **1977**, *16*, 1134.
(2) Datta, S.; McNeese, T. J.; Wreford, S. S. *Inorg. Chem.* **1977**, *16*, 2661.
(3) Casey, C. P.; Polichnowski, S. W. *J. Am. Chem. Soc.* **1977**, *99*, 6097.
(4) Hoffmann, R.; Beier, B. F.; Muetterties, E. L.; Rossi, A. R. *Inorg. Chem.* **1977**, *16*, 511.
(5) (a) Brown, L. D.; Datta, S.; Kouba, J. K.; Smith, L. K.; Wreford, S. S. *Inorg. Chem.* **1978**, *17*, 729. (b) Hawthorne, S. L.; Fay, R. C. *J. Am. Chem. Soc.* **1979**, *101*, 5268. (c) Bruder, A. H.; Fay, R. C.; Lewis, D. F.; Sayler, A. A. *Ibid.* **1976**, *98*, 6932. (d) Miessler, G. L.; Pignolet, L. H. *Inorg. Chem.* **1979**, *18*, 210.
(6) (a) Drew, M. G. B. *Prog. Inorg. Chem.* **1977**, *23*, 67. (b) Kepert, D. L. *Ibid.* **1979**, *25*, 41. (c) Steffen, W. L.; Chun, H. K.; Fay, R. C. *Inorg. Chem.* **1978**, *17*, 3498.
(7) Kouba, J. K.; Wreford, S. S. *Inorg. Chem.* **1976**, *15*, 1463.
(8) Colton, R.; Scollary, G. R.; Tomkins, I. B. *Aust. J. Chem.* **1968**, *21*, 15.
(9) Chen, G. J.-J.; Yelton, R. O.; McDonald, J. W. *Inorg. Chim. Acta* **1977**, *22*, 249.
(10) Templeton, J. L. *Adv. Chem. Ser.* **1979**, *No. 173*, 263.
(11) Colton, R.; Rix, C. J. *Aust. J. Chem.* **1969**, *22*, 305.

0020-1669/80/1319-1753$01.00/0

recorded on a Varian XL-100 spectrometer. Tris(acetylacetonato)chromium(III) (10 mg) was added to ^{13}C NMR samples as a shiftless paramagnetic relaxation agent. Low-temperature ^{13}C spectra were run in a solvent mixture of CD_2Cl_2:$CDCl_3$:CCl_4 (60:27:13) with Me_4Si as internal reference. Infrared spectra were recorded on a Beckman IR4250 spectrophotometer and calibrated with polystyrene.

$W(CO)_3(detc)_2$ (1). In a representative reaction, $W(CO)_4I_2$, 4.49 g (8.16 mmol), and sodium *N,N*-diethyldithiocarbamate (Na(detc)), 3.68 g (16.32 mmol), were combined in a 100-mL round-bottom flask under a nitrogen atmosphere. THF (20 mL) was then added via syringe; carbon monoxide evolution commenced and a red solution formed. After the solution was stirred for 1 h, the THF solvent was removed in vacuo. Addition of 20 mL of toluene resulted in a red slurry which was stirred under a carbon monoxide atmosphere for 5 min (the product reversibly loses carbon monoxide under vacuum[10]). The slurry was then chromatographed on an alumina column by using toluene as the eluant. The red-orange band was collected, and the solvent volume was reduced to 5 mL. Slow addition of 20 mL of cyclohexane to this concentrated solution and cooling of the solution to −20 °C for 12 h yielded orange-red crystals of $W(CO)_3(detc)_2$ (3.14 g (5.57 mmol), 68%). Crystalline $W(CO)_3(detc)_2$ is slightly air and moisture sensitive; the solid slowly turns green upon exposure to air for several days. Solutions are stable indefinitely under nitrogen and appear stable for several hours even upon exposure to air. ^1H NMR ($CDCl_3$): δ 1.22 (t, 12 H), 3.64 (q, 8 H). IR (toluene: ν_{CO} 2005, 1923, 1905 cm^{-1}.

$W(CO)_3(detc)_2$, ^{13}CO Enriched. A sample of $W(CO)_3(detc)_2$ was dissolved in toluene and held at a temperature of 40 °C under an atmosphere of labeled carbon monoxide (90% ^{13}C enriched) for 10 h. Crystallization, induced by the addition of cyclohexane, yielded approximately 40% ^{13}CO enriched as monitored by IR. Successive enrichment procedures resulted in approximately 90% ^{13}CO incorporation. IR (toluene): ν_{CO} 1999, 1983, 1970, 1920 (sh), 1898, 1880, 1865 (sh) cm^{-1}.

$W(CO)_3(dtc)_2$. Similar products were formed when $W(CO)_4I_2$ was allowed to react with other sodium *N,N*-dialkyldithiocarbamate (NaS_2CNR_2) salts. These products were observed by infrared spectroscopy and not characterized further for R = CH_2Ph (ν_{CO} 2020, 1931, and 1911 cm^{-1}) and R_2 = $(CH_2)_5$ (ν 2018, 1927, and 1908 cm^{-1}).

Crystals of $W(CO)_3(dmtc)_2$ (**2**) suitable for X-ray crystallographic analysis were grown over a 1-week period from a supersaturated toluene–cyclohexane solution.

Collection and Reduction of X-ray Data. Preliminary Weissenberg and precession photographs indicated that crystals of $W(CO)_3[S_2CNMe_2]_2$ (**2**) belonged to the monoclinic space group $C2/c$ or Cc as revealed by systematic absences for hkl ($h + k = 2n + 1$) and $h0l$ ($l = 2n + 1$). A dark orange-red crystal having dimensions 0.90 × 0.60 × 0.29 mm was selected and mounted, coated with epoxy, and used for subsequent diffractometer data collection. Observations were made by using graphite-monochromatized Mo $K\alpha_1$ (λ = 0.709 26 Å) radiation. The cell constants were obtained by least-squares refinement of 14 accurately centered reflections: a = 18.612 (3) Å, b = 6.313 (1) Å, c = 26.566 (5) Å, β = 93.76 (1)°. A calculated density of 2.18 g cm^{-3} with the assumption of eight molecules per unit cell compares with the observed flotation density of 2.14 (2) g cm^{-3} as measured in a mixture of bromoform and carbon tetrachloride. Using the experimental density and assuming only one molecule per asymmetric unit suggested that the space group $C2/c$ [C_{2h}^6; No. 15] be chosen for the initial refinement. This choice was later confirmed by successful refinement of the structure.

Intensity data were collected on a Picker four-circle automatic diffractometer at a takeoff angle of 1.8°. A θ–2θ scan mode over the range $3° \le 2\theta \le 60°$ at the rate of 1°/min with 10-s stationary-counter, stationary-crystal background counts at each end of the scan range was used to collect a total of 5902 reflections. A total of 3787 symmetry independent reflections having $F > 3\sigma(F)$ were used in the solution and refinement of the structure. As a general check on electronic and crystal stability, the intensities of three standard reflections ([11,3,2], [2,4,11], and [15$\bar{5}$]) were monitored at intervals of 97 reflections; no significant variation in intensity was observed during the data collection period for these three standards. The data were processed by using the formula of Ibers and co-workers[12] for the estimated standard deviation $\sigma(I) = [C + 0.25(t_s/t_b)^2(B_H + B_L) + p^2I^2]^{1/2}$; the value of p was assigned as 0.04.[13] The values I and $\sigma(I)$ were corrected for Lorentz–polarization effects by using the expression[14]

$$\frac{1}{Lp} = \frac{2 \sin 2\theta}{\cos^2 2\theta_m + \cos^2 2\theta}$$

where θ_m, the angle of the monochromator, was 11.63°.

Table I. Final Atomic Positional Parameters for $W(CO)_3[S_2CN(CH_3)_2]_2$[a]

atom	x	y	z
W	0.1060 (1)	0.0710 (1)	−0.1267 (1)
S(1)	0.1835 (1)	0.3500 (4)	−0.0840 (1)
S(2)	0.2277 (1)	−0.0791 (4)	−0.0963 (1)
S(3)	0.0917 (2)	−0.1895 (4)	−0.1987 (1)
S(4)	0.1688 (2)	0.2056 (5)	−0.2037 (1)
C(1)	0.0428 (5)	0.1752 (16)	−0.0758 (4)
O(1)	0.0039 (5)	0.2317 (15)	−0.0462 (4)
C(2)	0.0208 (6)	0.2031 (20)	−0.1660 (5)
O(2)	−0.0254 (5)	0.2757 (18)	−0.1887 (4)
C(3)	0.0708 (6)	−0.1740 (16)	−0.0898 (4)
O(3)	0.0512 (6)	−0.3204 (16)	−0.0692 (4)
C(4)	0.2532 (5)	0.1683 (14)	−0.0771 (3)
N(1)	0.3184 (4)	0.2164 (14)	−0.0578 (3)
C(5)	0.1393 (5)	−0.0180 (18)	−0.2345 (4)
N(2)	0.1521 (6)	−0.0610 (15)	−0.2813 (4)
C(6)	0.3367 (7)	0.4373 (16)	−0.0417 (5)
C(7)	0.3739 (7)	0.0551 (20)	−0.0513 (6)
C(8)	0.1236 (9)	−0.2530 (24)	−0.3078 (6)
C(9)	0.1927 (9)	0.0927 (23)	−0.3113 (6)

[a] Numbers in parentheses are the estimated standard deviations of the coordinates and refer to the last significant digit of the preceding number.

Solution and Refinement of the Crystal Structure. Examination of a three-dimensional Patterson function[15] yielded the positions of the tungsten and four sulfur atoms. Two cycles of full-matrix least-squares refinement were performed on these positions. All least-squares refinements in this study were carried out on F, the function minimized being $\sum w(|F_o| - |F_c|)^2$ where the weight, w, is taken as $4F_o^2/\sigma(F_o^2)$. When F_c was calculated, the atomic scattering factors for nonhydrogen atoms were taken from ref 16a. The effects of anomalous dispersion for tungsten and sulfur were also included in the calculation of F_c. Values of $\Delta f'$ and $\Delta f''$ were taken from ref 16b. The above refinement yielded values of the conventional residues R_1 = 0.267 and R_2 = 0.351, where $R_1 = \sum(|F_o| - |F_c|)/\sum|F_o|$ and $R_2 = [\sum w(|F_o| - |F_c|)^2/w(F_o)^2]^{1/2}$. The remaining nonhydrogen atoms were found from a difference Fourier synthesis. Anisotropic refinement of W and isotropic refinement of the remaining positions led to R_1 = 0.095 and R_2 = 0.122. Two cycles of anisotropic refinement for all nonhydrogen atoms lowered the residuals to R_1 = 0.084 and R_2 = 0.109.

At this stage of the refinement an absorption correction was applied (μ = 81.1 cm^{-1}), and eight low angle data which were suspected of flooding the counter were removed. Several more cycles of refinement led to convergence with discrepancy indices of R_1 = 0.070 and R_2 = 0.089. No atom parameter shifted by more than 0.20 times its estimated standard deviation during the final least-squares cycle. The ratio of data to variables was 22:1. The values of R_2 showed no unusual dependence on $|F|$ or sin θ, indicating our weighting scheme was appropriate. In the final difference Fourier synthesis a peak corresponding to 1.24 e $Å^{-3}$ was located approximately 1 Å from the center of the W atom, with all other electron densities less than 0.5 e $Å^{-3}$. The residual density due to the heavy transition metal is not unexpected and is presumably due to the inadequacy of our model for the tungsten electron density and the approximate nature of the absorption correction. The positional and thermal parameters derived from the last

(12) Corfield, P. W. R.; Doedens, R. J.; Ibers, J. A. *Inorg. Chem.* **1967**, *6*, 197.
(13) Busing, W. R.; Levy H. A. *J. Chem. Phys.* **1967**, *26*, 563.
(14) Goldfield, S. A.; Raymond, K. N. *Inorg. Chem.* **1971**, *10*, 2604.
(15) For a description of the programs used in this analysis, see: Lewis, D. L.; Hodgson, D. J. *Inorg. Chem.* **1974**, *13*, 143.
(16) Ibers, J. A., Hamilton, W. C., Eds. "International Tables for X-ray Crystallography"; Kynoch Press: Birmingham, England, 1974; Vol. IV: (a) Table 2.2A; (b) Table 2.3.1.

Table II. Final Anisotropic Thermal Parameters (10^2U_{ij}, Å^2) for $W(CO)_3[S_2CN(CH_3)_2]_2$[a]

atom	U_{11}	U_{22}	U_{33}	U_{12}	U_{13}	U_{23}
W	2.63 (2)	3.11 (2)	3.74 (2)	−0.10 (1)	−0.22 (1)	−0.04 (1)
S(1)	2.99 (10)	3.10 (10)	4.44 (12)	0.23 (8)	0.40 (9)	−0.41 (9)
S(2)	3.43 (11)	3.21 (11)	5.18 (14)	0.43 (9)	0.34 (10)	−0.44 (9)
S(3)	5.45 (15)	4.07 (13)	4.76 (14)	1.46 (11)	0.28 (11)	0.82 (10)
S(4)	4.75 (14)	4.67 (14)	4.36 (13)	1.31 (12)	0.04 (10)	0.06 (11)
C(1)	3.32 (45)	3.27 (49)	6.00 (64)	0.69 (37)	0.06 (41)	0.05 (41)
O(1)	4.23 (43)	6.53 (54)	8.05 (66)	0.57 (41)	2.09 (43)	0.31 (46)
C(2)	3.62 (49)	5.45 (64)	6.15 (70)	0.38 (48)	1.60 (46)	0.42 (52)
O(2)	5.51 (54)	7.55 (66)	9.37 (77)	0.88 (51)	2.46 (51)	1.32 (56)
C(3)	4.12 (52)	3.92 (54)	5.02 (58)	0.89 (41)	0.40 (42)	0.41 (41)
O(3)	6.60 (63)	5.38 (57)	10.45 (86)	0.01 (47)	2.91 (58)	2.38 (52)
C(4)	2.99 (40)	3.32 (44)	3.53 (44)	0.12 (33)	0.25 (32)	0.36 (33)
N(1)	2.82 (36)	4.42 (44)	4.65 (46)	0.22 (34)	0.40 (31)	0.04 (36)
C(5)	3.73 (46)	4.42 (50)	3.67 (46)	0.28 (42)	0.29 (37)	0.18 (39)
N(2)	5.70 (59)	5.71 (61)	3.80 (44)	0.35 (45)	0.44 (41)	0.42 (39)
C(6)	4.52 (59)	4.05 (56)	6.33 (71)	0.67 (44)	1.11 (51)	0.53 (46)
C(7)	3.57 (53)	5.86 (74)	7.08 (81)	0.88 (48)	1.07 (52)	0.75 (56)
C(8)	7.73 (93)	6.64 (82)	6.21 (82)	1.24 (72)	0.37 (68)	2.83 (67)
C(9)	6.93 (90)	7.05 (90)	5.44 (73)	0.45 (67)	2.09 (65)	0.86 (60)

[a] The form of the anisotropic temperature factor is $\exp[-2\pi^2(U_{11}h^2a^{*2} + U_{22}k^2b^{*2} + U_{33}l^2c^{*2} + 2U_{12}hka^*b^* + 2U_{13}hla^*c^* + 2U_{23}klb^*c^*)]$.

Table III. Intramolecular Bond Distances (Å) for $W(CO)_3[S_2CN(CH_3)_2]_2$

A. Tungsten Coordination Sphere

W-S(1)	2.501 (2)	W-C(1)	1.964 (11)
W-S(2)	2.538 (3)	W-C(2)	2.021 (10)
W-S(3)	2.523 (3)	W-C(3)	1.966 (11)
W-S(4)	2.569 (3)		

B. *N*,*N*-Dimethyldithiocarbamate and Carbon Monoxide Ligands

S(1)-C(4)	1.732 (9)	C(4)-N(1)	1.321 (12)
S(2)-C(4)	1.701 (9)	C(5)-N(2)	1.308 (14)
S(3)-C(5)	1.726 (11)	N(1)-C(6)	1.491 (13)
S(4)-C(5)	1.704 (11)	N(1)-C(7)	1.453 (14)
C(1)-O(1)	1.161 (13)	N(2)-C(8)	1.482 (16)
C(2)-O(2)	1.115 (13)	N(2)-C(9)	1.493 (16)
C(3)-O(3)	1.146 (14)		

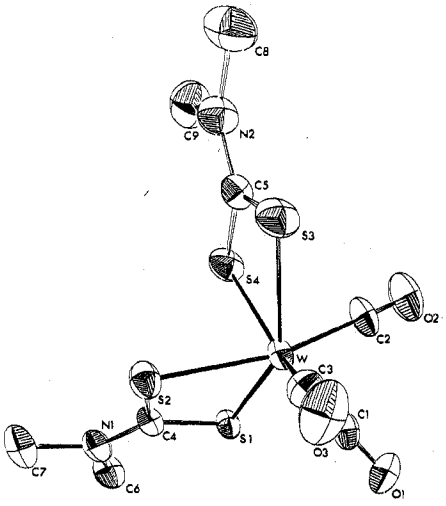

Figure 1. Perspective view of **2** showing the atomic labeling scheme and illustrating the 4:3 geometry displayed by [C(1),C(3),S(1),S(2)]:[C(2),S(3),S(4)]. Thermal ellipsoids are drawn at the 50% probability level.

cycle of least-squares, along with the standard deviations as estimated from the inverse matrix, are located in Tables I and II. A table of observed and calculated structure amplitudes is available as supplementary material.

Results

The molecular structure of **2** is illustrated in Figure 1. The contents of the unit cell are presented in the packing diagram of Figure 2. The structure consists of well-separated mono-

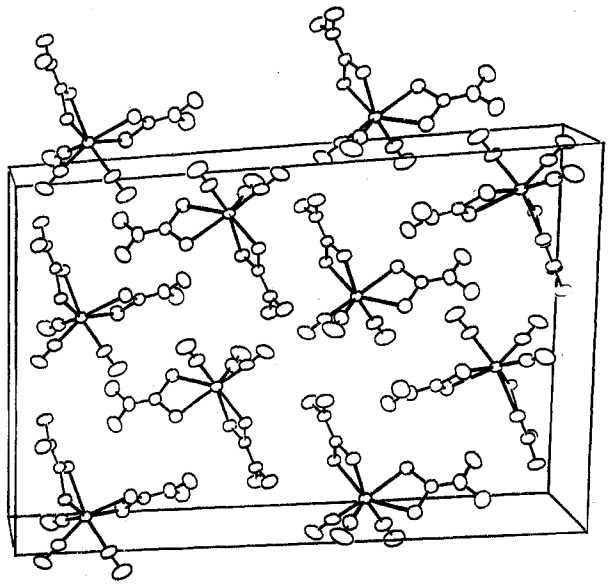

Figure 2. A view of the unit cell contents of **2**.

Table IV. Intramolecular Bond Angles (Deg) for $W(CO)_3[S_2CN(CH_3)_2]_2$

A. Tungsten Coordination Sphere Angles

C(1)-W-C(3)	71.7 (4)	C(2)-W-S(1)	110.7 (4)
C(1)-W-C(2)	74.4 (5)	C(2)-W-S(3)	80.6 (4)
C(1)-W-S(1)	78.8 (3)	C(2)-W-S(2)	166.4 (4)
C(1)-W-S(3)	134.6 (3)	C(2)-W-S(4)	80.5 (4)
C(1)-W-S(2)	118.1 (3)	S(1)-W-S(3)	146.3 (1)
C(1)-W-S(4)	139.7 (3)	S(1)-W-S(2)	69.1 (1)
C(3)-W-C(2)	107.8 (5)	S(1)-W-S(4)	81.3 (1)
C(3)-W-S(1)	122.0 (3)	S(2)-W-S(3)	92.6 (1)
C(3)-W-S(3)	80.9 (3)	S(2)-W-S(4)	86.1 (1)
C(3)-W-S(2)	82.4 (3)	S(3)-W-S(4)	69.0 (1)
C(3)-W-S(4)	147.3 (3)		

B. Ligating Atom Angles

W-C(1)-O(1)	177.9 (1.2)	W-S(2)-C(4)	88.8 (3)
W-C(2)-O(2)	178.8 (1.4)	W-S(3)-C(5)	88.7 (4)
W-C(3)-O(3)	178.5 (1.2)	W-S(4)-C(5)	87.7 (4)
W-S(1)-C(4)	89.2 (3)		

C. *N*,*N*-Dimethyldithiocarbamate Angles

S(1)-C(4)-N(1)	123.4 (7)	C(4)-N(1)-C(6)	120.9 (9)
S(2)-C(4)-N(1)	124.0 (7)	C(4)-N(1)-C(7)	120.8 (9)
S(3)-C(5)-N(2)	121.7 (9)	C(5)-N(2)-C(8)	122.6 (1.1)
S(4)-C(5)-N(2)	123.7 (9)	C(5)-N(2)-C(9)	120.2 (1.0)

Table V. Least-Squares Planes Atomic Coordinates for $W(CO)_3[S_2CN(CH_3)_2]_2$

atom	x	y	z	Δ, Å
		Plane 1		
C(1)	0.932	1.102	−2.008	−0.034
C(3)	1.485	1.109	−2.373	0.033
S(1)	3.564	2.211	−2.227	0.028
S(2)	4.410	−0.500	−2.554	−0.027
		Plane 2		
W	2.195	0.448	−3.358	0.04
C(1)	0.932	1.102	−2.008	0.84
C(3)	1.485	−1.109	−2.373	−0.59
S(1)	3.564	2.211	−2.227	−0.53
S(3)	2.056	−1.199	−5.265	0.01
S(4)	3.501	1.297	−5.400	0.23

Table VI. Dihedral Angle Calculations[a] for Comparison of $W(CO)_3[S_2CN(CH_3)_2]_2$ with Various Trial Geometries[b]

trial geometry	dihedral angles, deg: δ_i(obsd)	δ_i(idealzd)
4:3 (piano stool), C(1)C(3)S(1)S(2):C(2)S(3)S(4)	1.1, 3.8	0, 0
1:4:2 (capped trigonal prism), S(4):C(2)S(1)S(2)S(3):C(1)C(3)	48.7, 24.4, 3.8	41.5, 0, 0
1:3:3 (capped octahedron), C(3):C(1)S(2)S(3):C(2)S(1)S(4)	48.7, 19.0, 3.8	24.2, 24.2, 24.2

[a] The dihedral angles were calculated following projection of the ligating atoms onto a sphere of unit radius. [b] See text for a description of and references to the idealized geometries and corresponding δ_i values.

mers of tricarbonylbis(*N*,*N*-dimethyldithiocarbamato)tungsten(II), with one molecule per asymmetric unit of the C-centered monoclinic cell. Intramolecular bond lengths and bond angles are listed in Tables III and IV, respectively. Table V lists important least-squares planes, and Table VI presents dihedral angles between several planes, each of which is defined by three ligating atoms. There are no unusual intermolecular nonbonded contacts in the unit cell.

Variable-temperature carbon-13 NMR spectra for **1** are reproduced in Figure 3. Chemical shifts and relevant coupling constants are listed in Table VII.

Discussion

Description of the Molecular Structure of 2. The molecular structure of $W(CO)_3(dmtc)_2$ confirms that both dithiocarbamate ligands chelate the metal ion to form a heptacoordinate tungsten(II) complex. The tungsten coordination sphere is constructed in a manner which places the three carbon monoxide ligands in a cis arrangement relative to one another, the arrangement required in order to minimize competition for π electron density available from the d^4 metal ion.

The geometries adopted by the bidentate dithiocarbamate ligands are normal for these groups. The observed S–S bites of 2.86 Å for S(1)–S(2) and 2.89 Å for S(3)–S(4) are similar to values reported for other dithiocarbamate complexes of heavy transition metals from the early portion of the periodic chart.[6] The S_2CNC_2 framework of each chelate is planar within experimental error. Considerable double bond character is reflected in the average length of 1.31 Å for the N(1)–C(4) and N(2)–C(5) bonds which compares to the average of the four methyl–nitrogen bond lengths of 1.48 Å, a value typical of carbon–nitrogen single bonds.[17] Delocalization of π electron density over the S_2CN moiety indeed strengthens the C–N linkage and effectively inhibits rotation of the NMe_2 group at room temperature and below for NMR purposes, but the observed carbon–nitrogen bond lengths are still somewhat longer than the 1.27 Å length associated with simple C=N bonds.[17]

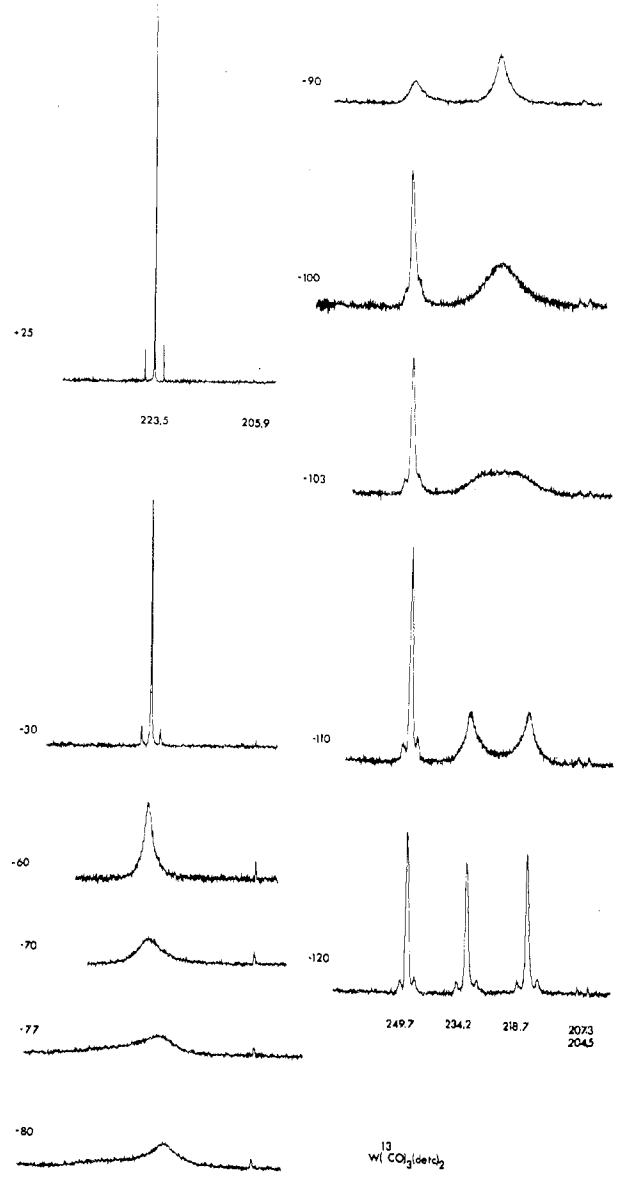

Figure 3. Variable-temperature $^{13}C\{^1H\}$ NMR spectra of ^{13}CO-enriched **1** in the low-field region displaying resonances due to ^{13}CO and naturally abundant $Et_2N^{13}CS_2^-$ (chemical shifts are listed in ppm downfield from Me_4Si).

Table VII. Carbon-13 NMR Data[a]

compd	^{13}C	35 °C	−78 °C	−120 °C
1	$-CH_3$	12.5	12.5	12.4
	$-CH_2-$	44.5	44.4	44.5
	R_2NCS_2	206.4	206.4	204.5
				207.3
	CO	233.5 (119)	227	218.7 (133)
			250	234.2 (133)
				249.7 (91)
2[b]	$-CH_3$	39.2	39.2	38.4
				39.4
	R_2NCS_2	208.7	206	203.7
				206.3
	CO	233.1 (119)	226	218.2
			248	233.2
				248.8

[a] Chemical shifts in ppm relative to Me_4Si ($^1J(^{183}W-^{13}C)$ in Hz). [b] Data for compound **2** are taken from ref 10.

(17) Pauling, L. "The Nature of the Chemical Bond", 3rd ed.; Cornell University Press: Ithaca, N.Y., 1960.

The average W–S bond length of 2.53 Å found here is similar to the average of 2.52 Å reported for the four W–S distances in $W(CO)(HC{\equiv}CH)(detc)_2$.[18] Higher oxidation state tungsten dithiocarbamate complexes have been studied which exhibit average W–S distances of 2.48 and 2.51 Å for W(IV) and W(V), respectively.[19] A number of structural determinations have been reported for molybdenum dithiocarbamate complexes, and a wide variation in metal–sulfur bond lengths has been obtained. An example of the flexibility of the molybdenum–dithiocarbamate bond is provided by the bis(phenylnitrene) complex *cis*-$Mo(NPh)_2(detc)_2$ which exhibits Mo–S distances of 2.45, 2.46, 2.60, and 2.76 Å.[20]

The average W–C bond length of 1.98 Å is typical of tungsten(II)–carbonyl complexes (cf. an average of 1.95 Å for 15 independent W–C distances determined for $W(CO)_3(dmpe)I_2$[21]). The range of molybdenum- and tungsten–carbon distances characterizing heptacoordinate d^4 monomeric carbonyls is quite small.[6] Within the set of three metal–carbon monoxide bond distances reported here for **2** the W–C(2) length (2.021 Å) is unique, differing by roughly 5σ from the other two W–C separations which are experimentally equivalent (1.964 and 1.966 Å). While it is tempting to associate C(2) with certain distinct NMR properties exhibited by one of the three carbon monoxide ligands on this basis (vide infra), it is well established that structural artifacts can occur in heavy metal–carbonyl complexes which produce deceptive metal–carbon distances.[22] Comparison of metal–oxygen distances often provides a more significant measure of variation in metal–carbon monoxide bonding than M–C bond lengths since the position of carbon along the MCO axis may not be well-defined.[23] In the case of **2** the W–O(2) distance is indeed the longest of the three, but the range of W–O differences is less than 0.03 Å and hence less than 3σ. A more substantive basis for assigning the roles of the respective carbon monoxide ligands in the dynamic behavior of **1** and **2** stems from analysis of the coordination geometry as described below.

The bite angles of 69.1 and 69.0° which are the result of W–S bond lengths ranging between 2.50 and 2.57 Å coupled with the fixed ligand configuration (a normalized bite of (S···S)/(W···S) = 1.14) impose certain restrictions on the coordination geometry about tungsten. There has been general agreement in the literature that visual inspection of seven-coordinate structures rarely provides an adequate description of the geometry.[24] Quantitative assessments of the relationship between the observed disposition of ligands and idealized polygons have been proposed which eliminate some, but not all, of the ambiguities surrounding seven-coordination shapes. The method presented by Muetterties and Guggenberger relies on dihedral angles (δ_i) between adjacent triangular faces defined by ligating atoms to parameterize ML_7 shapes.[25] Alternatively one can normalize all metal–ligand bond distances prior to performing dihedral angle calculations.[7,21] Neither approach provides a unique description for an experimentally determined heptacoordinate complex, but either analysis is superior to visual inspection alone. Indeed no inescapable correlation between the structure of **2** and any of the three idealized geometries is evident from any perspective.

Least-squares-planes calculations involving the seven atoms in the inner coordination sphere identified C(1)–C(3)–S(1)–S(2) as the only set of more than three atoms approximating a plane (an average deviation of ±0.03 Å). No group of five ligating atoms was close to coplanarity, thus excluding the 1:5:1 geometry from further consideration. Indeed no angle of 180° as required for the two axial ligands of an ideal pentagonal bipyramid is present in the structure of **2**. The largest ligand–metal–ligand angle is 166.4° for C(2)–W–S(2) with 146.3° for S(1)–W–S(3) second largest. Assuming then that a 1:5:1 structure would logically involve C(2) and S(2) as axial ligands necessarily leaves a girdle consisting of C(1), C(3), S(1), S(3), and S(4) with a large average deviation from planarity of 0.45 Å; i.e., the pentagonal bipyramid is clearly an inadequate description of the geometry found for **2**.

Although the 4:3 "piano stool" geometry has not been a popular choice as one of the basic idealized forms to be used for describing seven-coordinate structures due to the close similarity between a plane of four donor atoms parallel to a plane of three donor atoms and certain orientations of either a capped octahedron or a capped trigonal prism,[6] the planarity of C(1)–C(3)–S(1)–S(2) in **2** suggests that the idealized 4:3 geometry be considered either independently or as a point of departure for other standard geometries.

Viewing **2** as a 4:3 system, [C(1), C(3), S(1), S(2)]:[C(2), S(3), S(4)], the observed angle between the two ligating atom planes is 13.4°. Normalization of metal–ligand bond lengths by projection onto a sphere of unit radius results in an angle of only 1.1° between these two planes of the 4:3 geometry, nearly identical with the ideal value of 0°. Dreyer, Lam, and Lippard have recently reported that the 4:3 description of $(RNC)_3W(CO)_2I_2$ is preferable to the usual polygonal alternatives.[26] With 0° as the criteria both for the angle between the two planes and for the dihedral angle across the diagonal of the quadrilateral face, the values of 1.1 and 3.8°, respectively, which characterize **2** indicate the compatibility of the observed structure with the tetragonal base–trigonal base geometry.

One can employ the correspondence between 4:3 and 1:3:3 or 1:4:2 geometries suggested by Drew[6] to calculate the relevant δ' angles for describing **2** as a capped octahedron or as a capped trigonal prism. The δ' values listed in Table VI indicate that the observed structure most nearly approximates the 4:3 geometry. It should be noted that the distribution of ligands into the tetragonal plane and the trigonal plane is not based on grouping identical atoms together in either **2** or $(RNC)_3W(CO)_2I_2$;[26] i.e., the 4:3 classification is not $S_4{:}C_3$ for **2** nor is it $(CO)_2I_2{:}(CNR)_3$ for $(RNC)_3W(CO)_2I_2$. If an assignment to one of the three standard shapes is based on the experimental δ' values, the capped trigonal prism with S(4) capping is superior to alternative choices. Furthermore, the choice of δ_1' is not unique and the average δ_1' of 37.8° (48.7° for S(4)S(2)S(3)/S(2)S(3)C(3) and 26.8° for S(4)S(1)C(2)/S(1)C(2)C(1)) approaches the theoretical 41.5° calculated for an undistorted capped trigonal prism. The large difference between the two δ_1' angles reflects a departure of the S(4) position from the center of the capped quadrilateral face which is imposed by the rigid S(3)–S(4) bite.

Metal–ligand bond lengths are compatible with either the 4:3 or the 1:4:2 description. The two carbonyls with equivalent bond lenths (C(1) and C(3)) are both found in the tetragonal base of the 4:3 or the uncapped edge of the 1:4:2. Either description leaves C(2) as the unique carbonyl ligand. The longest metal–sulfur distance, 2.569 (3) Å, connects the capping ligand of the trigonal prism, S(4), to tungsten.

(18) Ricard, L.; Weiss, R.; Newton W. E.; Chen, G. J.-J.; McDonald, J. W. *J. Am. Chem. Soc.* **1978**, *100*, 1318.
(19) Bino, A.; Cotton, F. A.; Dori, Z.; Sekutowski, J. C. *Inorg. Chem.* **1978**, *17*, 2946.
(20) Haymore, B. L.; Maatta, E. A.; Wentworth, R. A. D. *J. Am. Chem. Soc.* **1979**, *101*, 2063.
(21) Drew, M. G. B.; Rix, C. J. *J. Organomet. Chem.* **1975**, *102*, 467.
(22) (a) Goldberg, S. Z.; Raymond, K. N. *Inorg. Chem.* **1973**, *12*, 2923. (b) Mawby, A.; Pringle, G. E. *J. Inorg. Nucl. Chem.* **1972**, *34*, 517.
(23) Drew, M. G. B.; Wilkins, J. D. *J. Organomet. Chem.* **1974**, *69*, 271.
(24) Muetterties, E. L.; Wright, C. M. *Q. Rev., Chem. Soc.* **1967**, *21*, 109.
(25) Muetterties, E. L.; Guggenberger, L. J. *J. Am. Chem. Soc.* **1974**, *96*, 1748.
(26) Dreyer, E. B.; Lam, C. T.; Lippard, S. J. *Inorg. Chem.* **1979**, *18*, 1904.

Table VIII. Activation Barriers Calculated for $W(CO)_3[S_2CNR_2]_2$ Complexes[a]

complex	^{13}C probe	$\Delta G^{\ddagger}$, kcal mol^{-1}
1	R_2NCS_2	8.5 ± 0.1[b]
	*C*O (3-site exchange)	8.5 ± 0.1
	*C*O (2-site exchange)	7.5 ± 0.1
2[c]	$-CH_3$	9.0 ± 0.1
	R_2NCS_2	9.0 ± 0.1
	*C*O (3-site exchange)	9.0 ± 0.1
	*C*O (2-site exchange)	8.1 ± 0.1

[a] See text and ref 10 for details of the $\Delta G^{\ddagger}$ calculation. [b] The ± values following $\Delta G^{\ddagger}$ serve only as an indication of the agreement for determinations at various temperatures and do not represent error limits. [c] Data for compound **2** are taken from ref 10.

Dynamic Properties of 1 and 2 in Solution. The dynamic properties of **1** and **2** are very similar as reflected by variable temperature ^{13}C NMR studies. The chemical shifts and coupling constants (Table VII) as well as the activation barriers (Table VIII) calculated for the (*N*,*N*-dimethyldithiocarbamato)- and the (*N*,*N*-diethyldithiocarbamato)tungsten(II) rearrangements are qualitatively very similar, and the assumption that the same mechanism is applicable in both cases seems well-founded. Furthermore the location of the methyl groups in the structure of **2** is such that it seems unlikely that the coordination geometry at the metal center would be significantly altered by ethyl substitution. In view of the above considerations and in order to facilitate discussion of the dynamic ^{13}C NMR spectra, we will assume for the remainder of the analysis that the structure and the stereochemical nonrigidity of **1** and **2** are indeed similar.

The greater solubility of **1** (as compared to **2**) coupled with the ease of ^{13}CO enrichment in these $W(CO)_3(dtc)_2$ complexes allowed us to obtain useful ^{13}C NMR data from ambient temperature down to −120 °C. The observation of a single carbonyl resonance at room temperature (Figure 3) is incompatible with virtually any conceivable static seven-coordinate geometry in the absence of accidental chemical shift degeneracies. Indeed the limiting low-temperature spectrum of **1** displays three distinct carbonyl signals of equal intensity in accord with a static structure equivalent to the geometry determined for **2** in the solid state where each carbon monoxide ligand is located in a unique molecular environment.

Stereochemical nonrigidity is a well-documented characteristic of both heptacoordinate complexes[27] and $M(CO)_3$ fragments.[28] Most monomeric complexes containing a metal–tricarbonyl moiety which have been studied by dynamic ^{13}C NMR produce a low-temperature limiting spectrum consisting of two signals with an intensity ratio of 2:1.[29] Several unsymmetrical (diene)iron–tricarbonyl compounds which have been investigated display three independent carbon monoxide ^{13}C resonances in the low-temperature limit.[30] Regardless of the number of unique resonances associated with the static structure, the dynamic behavior of each of the monomeric complexes cited is compatible with a single process simultaneously averaging the three carbon monoxide signals.

The $W(CO)_3(dtc)_2$ compounds provide a somewhat unique example of $M(CO)_3$ fluxionality in monomeric complexes in that the single carbonyl resonance recorded at high temperature broadens progressively with decreasing temperature until two signals are evident with a 2:1 intensity ratio. However, upon further cooling, the downfield signal of unit intensity continues to sharpen while the doubly intense upfield resonance undergoes an increase in width and eventually splits into two equiintensity absorptions. This sequence of NMR events as a function of temperature is clearly indicative of two distinct dynamic processes. The single resonance attributable to the central dithiocarbamate carbon also broadens and separates into two independent signals over this temperature range.

Activation barriers for the two exchange processes reflected in the carbon-13 spectra of both **1** and **2** were calculated from the Eyring equation after k_{ex} was determined by the Gutowsky–Holm equation at the coalescence temperature,[31] and the fast- and slow-exchange approximations[32] were employed when appropriate[33] as discussed in detail previously.[10] The resulting $\Delta G^{\ddagger}$ values are listed in Table VIII.

The possibility that dissociative loss of carbon monoxide, clearly a facile process based on the mild conditions suitable for incorporation of the carbon-13 label, might play a role in dynamics of **1** on the NMR time scale was eliminated by observation of ^{183}W–^{13}C satellites (^{183}W ($I = {}^1/_2$), 14.4% natural abundance) in the high-temperature spectrum. The retention of coupling information ($^4J(^{183}W$–$^{13}C) = 119$ Hz) provides definitive evidence for an intramolecular rearrangement process. The observed coupling constant is necessarily an average of the three independent values characterizing the static solution structure. The signal-to-noise ratio obtained in the limiting low-temperature spectrum of **1** was adequate to resolve each of the three tungsten–carbon coupling constants: 91, 133, and 133 Hz for the three distinct carbonyl signals at 249.7, 234.2, and 218.7 ppm, respectively. A survey of the $^1J(^{183}W$–$^{13}C)$ values tabulated by Todd and Wilkinson[34] suggests that the 91-Hz coupling observed for the low-field carbonyl is abnormally small while the 133-Hz ^1J values are in the range typical of W–C coupling constants in tungsten–carbonyl complexes. Chemical intuition suggests that one might logically associate a smaller coupling constant with a weaker metal–ligand bond. While the existing data base is not large enough to confirm such a conclusion, comparison of germane cis and trans coupling constants for $(R_3P)W(CO)_5$ complexes, where the trans carbonyl is generally conceded to be more tightly bound than the four cis ligands, does support the above correlation since the trans W–C coupling constant is invariably 10–20 Hz larger than the cis.[34]

Identification of the unique carbonyl ligand, i.e., the one not involved in the low-energy rearrangement process, can be based on both the position and bonding of the three carbonyl ligands in the tungsten coordination sphere. Assuming that the crystal structure of **2** provides a good model for the static solution structure of both **1** and **2** allows one to consider the mechanistic implications of the observed fluxionality as follows. The location of C(2) in the trigonal base of the 4:3 geometry sets it apart from the remaining two carbon monoxide ligands. If one considers the best standard geometrical description, the same conclusion results since C(2) stands alone as a carbonyl ligand on the capped face while both C(1) and C(3) occupy the uncapped edge of the optimal capped trigonal prism description.

As noted during the structural discussion, the W–C(2) bond length, although not the best absolute indicator of metal–ligand

(27) (a) Albright, J. O.; Datta, S.; Dezube, B.; Kouba, J. K.; Marynick, D. S.; Wreford, S. S.; Foxman, B. M. *J. Am. Chem. Soc.* **1979**, *101*, 611. (b) Given, K. W.; Mattson, B. M.; Pignolet, L. H. *Inorg. Chem.* **1976**, *15*, 3152. (c) Bhat, A. N.; Fay, R. C.; Lewis, D. F.; Lindmark, A. F.; Strauss, S. H. *Ibid.* **1974**, *13*, 886.
(28) (a) Kreiter, C. G.; Lang, M. *J. Organomet. Chem.* **1973**, *55*, C27. (b) Kruczynski, L.; Takats, J. *J. Am. Chem. Soc.* **1974**, *96*, 932. (c) Cotton, F. A.; Hanson, B. E. *Isr. J. Chem.* **1977**, *15*, 165.
(29) (a) Lallemand, J. Y.; Laszlo, P.; Musette, C.; Stockis, A. *J. Organomet. Chem.* **1975**, *91*, 71. (b) Cotton, F. A.; Hunter, D. L. *J. Am. Chem. Soc.* **1976**, *98*, 1413.
(30) Kreiter, C. G.; Stuber, S.; Wackerle, L. *J. Organomet. Chem.* **1974**, *66*, C49.
(31) Gutowsky, H. S.; Holm, C. H. *J. Chem. Phys.* **1956**, *25*, 1228.
(32) Anet, F. A. L.; Bourn, A. J. R. *J. Am. Chem. Soc.* **1967**, *89*, 760.
(33) Faller, J. W. *Adv. Organomet. Chem.* **1977**, *16*, 211.
(34) Todd, L. J.; Wilkinson, J. R. *J. Organomet. Chem.* **1974**, *77*, 1.

Scheme I

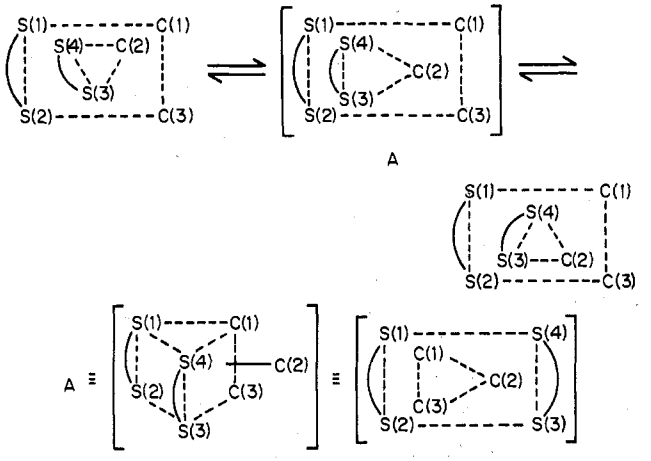

bond strength, is indeed longer than the corresponding bonds to C(1) and C(3), and hence this criterion also supports assignment of the low-field ^{13}C NMR signal to the C(2) carbonyl based on the small coupling constant. The above factors lead us to conclude that C(2) remains unique during the fluxional process responsible for averaging C(1) and C(3) at low temperatures and only enters into the dynamic NMR arena with the onset of the higher energy exchange phenomenon. Similar dynamic behavior has been reported for an $M(CO)_3$ fragment in iron–carbonyl dimers where one of the two $Fe(CO)_3$ moieties present undergoes two separate rearrangements to account for three low-temperature signals initially coalescing to two (2:1 intensity ratio) before complete averaging of the three occurs to produce a single line.[35]

One simple physical motion which could account for equilibration of the magnetic environments of C(1) and C(3) involves twisting the trigonal plane relative to the tetragonal base as depicted in Scheme I. A series of such rotations would interconvert the two equienergetic permutational isomers and average NMR signals C(1) and C(3) without altering the C(2) resonance. Furthermore the two dithiocarbamate ligands remain distinct, one in the tetragonal plane and one in the trigonal plane, in accord with the observation of two separate signals for the central carbon of these chelates in the low-temperature region (vide infra).

The postulated twisting motion requires that a symmetric 4:3 geometry of the type illustrated in Scheme I be realized during the transformation relating the two permutational isomers. If the rearrangement is rapid on the NMR time scale, the effective geometry becomes that of the symmetrical intermediate even though no such isomer is ever significantly populated at any temperature. This intermediate will actually approximate a canonical 4:3 distribution of the ligands; i.e., S_4:C_3 will pertain as well as the original C(1)C(3)S(1)S(2):C(2)S(3)S(4) classification. Alternatively one can view the time-averaged structure as a capped trigonal prism with C(2) the capping ligand so that a plane of symmetry relates

Scheme II

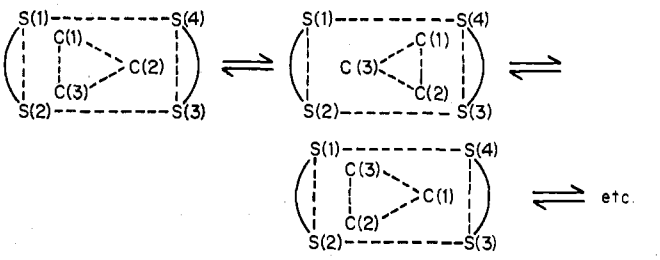

S(1) to S(2), S(3) to S(4), and C(1) to C(3) while C(2) is unique and lies within the molecular mirror plane. This postulated low-energy fluxional process then averages C(1) and C(3) while allowing the dithiocarbamate carbons and C(2) to remain unique in accord with the experimental data.

The molecular rearrangement occurring at higher temeratures can be formulated in terms of the C_s symmetry which is operative due to prior implementation of the low-energy fluxionality. Cyclic permutation of the three carbon monoxide ligands could be accomplished by internal rotation of the tricarbonyl fragment relative to the rest of the molecule. This simple rotary process has not been proven to be the actual physical phenomenon which is responsible for the local scrambling common to many $M(CO)_3$ moieties, but it provides the simplest description consistent with numerous experimental obervations to date.[36] When one realizes that the S_4:C_3 ligand distribution to form a 4:3 geometry allows the realization of an equivalent permutational isomer with every 60° rotation as well as at 120° rotations, it is clear that the two dithiocarbamate environments will also be averaged by rotation of the tricarbonyl fragment. The observed coalescence of the central dithiocarbamate carbon signals is compatible with this mechanistic possiblity (Scheme II). This same rotation would be expected to average all of the alkyl environments as is observed experimentally.[10] The agreement evident among interconversion barriers calculated independently from the dithiocarbamate carbon-13 data and the high-temperature carbon monoxide data support the hypothesis that the same intramolecular mechanism is responsible for the dynamic NMR properties which are probed at multiple sites in the complex.

Acknowledgment. The authors are grateful to Dr. E. J. Valente and Mr. S. B. Wilson for providing expert crystallographic assistance. This work was supported by a generous grant from the North Carolina Science and Technology Committee and a Cottrell Research Grant from the Research Corp.

Registry No. **1**, 72827-54-4; **2**, 72881-01-7; $W(CO)_4I_2$, 40813-52-3; $W(CO)_3[S_2CN(CH_2Ph)_2]_2$, 72827-55-5; $W(CO)_3[S_2CN(CH_2)_5]_2$, 72827-56-6.

Supplementary Material Available: A listing of observed and calculated structure amplitudes (21 pages). Ordering information is given on any current masthead page.

(35) (a) Cotton, F. A.; Hunter, D. L.; Lahuerta, P. *J. Am. Chem. Soc.* **1975**, *97*, 1046. (b) Cotton, F. A.; Hunter, D. L. *Ibid.* **1975**, *97*, 5739.

(36) (a) Cotton, F. A.; Hunter, D. L.; Lahuerta, P. *Inorg. Chem.* **1975**, *14*, 511. (b) Aime, S.; Milone, L.; Sappa, E. *J. Chem. Soc., Dalton, Trans.* **1976**, 838.